Kondo ground states and non-Fermi-liquid behavior in $CeNi_{1-x}Co_xGe_2$

B. K. Lee, J. B. Hong, J. W. Kim, Kwang-hyun Jang, and E. D. Mun
BK21 Physics Research Division and Institute of Basic Science, Sungkyunkwan University, Suwon 440-746, South Korea

M. H. Jung
National Research Laboratory for Material Science, Korea Basic Science Institute (KBSI), 52 Yeoeun-Dong Yusung-Gu, Daejeon, 305-333 South Korea

S. Kimura
UVSOR Facility, Institute for Molecular Science, Okazaki 444-8585, Japan

Tuson Park
Los Alamos National Laboratory, Los Alamos, New Mexico 87545, USA

J.-G. Park
BK21 Physics Research Division and Institute of Basic Science, Sungkyunkwan University, Suwon 440-746, South Korea and Center for Strongly Correlated Materials Research, Seoul National University, Seoul 151-742, South Korea

Y. S. Kwon*
BK21 Physics Research Division and Institute of Basic Science, Sungkyunkwan University, Suwon 440-746, South Korea, UVSOR Facility, Institute for Molecular Science, Okazaki 444-8585, Japan and Center for Strongly Correlated Materials Research, Seoul National University, Seoul 151-742, South Korea

(Received 10 July 2004; revised manuscript received 27 December 2004; published 30 June 2005)

We report measurements of the magnetic susceptibility, specific heat, and electrical resistivity of the heavy fermion alloy series $CeNi_{1-x}Co_xGe_2$. With increasing x, hybridization between the localized $4f$ and conduction band electrons is enhanced. The magnetic order observed at $x=0$ is completely suppressed at $x=0.3$ and non-Fermi-liquid behavior appears at the critical concentration, which is analyzed in terms of two-dimensional antiferromagnetic quantum fluctuations. Specific heat and magnetic susceptibility data are quantitatively explained by the Coqblin-Schrieffer model with degenerate impurity spin $j=1/2$, $3/2$, and $5/2$ for Co concentration range of $x \leqslant 0.6$, $0.7 \leqslant x \leqslant 0.8$, and $x \geqslant 0.9$, respectively.

DOI: 10.1103/PhysRevB.71.214433 PACS number(s): 75.30.Mb, 75.20.Hr

I. INTRODUCTION

Ce-based ternary intermetallic compounds have been the subject of continuous interest because of their interesting ground states. These compounds have a localized $4f$ electron for each Ce^{3+} ion. Upon cooling, several magnetic ground states are realized due to competition between Kondo and RKKY (Ruderman-Kittel-Kasuya-Yosida) interactions.[1–3] The energy scales for the Kondo singlet and the magnetically ordered state depend on hybridization strength $|JN_F|$ between the localized f states and conduction-electron states, i.e., $T_K \propto \exp(-1/JN_F)$ and $T_{\mathrm{RKKY}} \propto J^2 N_F$, where J is the exchange coupling parameter and N_F is the density of states at the Fermi level. A local-moment magnetism (LMM) for a small value of $N_F J$ is stabilized, while an intermediate-valence (IV) behavior is anticipated for a large value of $N_F J$. Heavy-fermion (HF) behavior is often observed at the borderline between the LMM and IV regime.

Recently several heavy fermion compounds have been reported to show deviation from Fermi-liquid theory, so-called non-Fermi liquid (NFL) behavior in the vicinity of magnetic quantum critical point where Néel (T_N) or Curie temperature (T_C) is suppressed to 0 K. Such NFL behavior can be characterized as follows: electrical resistivity $\rho \propto T^n$ with $n<2$ and magnetic susceptibility $\chi \propto T^{-1+\lambda}$ with $\lambda<1$ or $\chi_0(1-aT^{1/2})$. Specific heat divided by temperature follows either a logarithmic temperature dependence $C/T \propto -\ln T$ or a power law behavior $C/T \propto T^{-1+\lambda}$. Several scenarios have been put forward to explain the NFL behavior; (i) a multichannel Kondo impurity model in which more than one channel of conduction electrons are antiferromagnetically coupled to an impurity spin,[4,5] (ii) a disorder-induced distribution of the Kondo temperature,[6,7] (iii) a second-order quantum phase transition to a magnetic state at a quantum-critical point (QCP),[8–10] and (iv) a Griffiths phase which is characterized by magnetic clusters in a nonmagnetic background.[11,12]

In this paper, we report results of electrical resistivity, magnetic susceptibility, and specific heat of the series of intermetalic compounds $CeNi_{1-x}Co_xGe_2$ ($0 \leqslant x \leqslant 1$). Unlike other ternary compounds, the lattice parameter is essentially independent of the amount of Co doping x. $CeNiGe_2$ ($x=0$) is a heavy-fermion compound with an antiferromagnetic order below 4.2 K (Ref. 13) while $CeCoGe_2$ ($x=1$) is a nonmagnetic heavy-fermion Kondo compound with $j=5/2$ ground state and large Kondo temperature $T_K > 200$ K.[14,15] At $x=0.3$, T_N is suppressed below the lowest temperature (0.5 K) that we can measure down to and non-Fermi-liquid

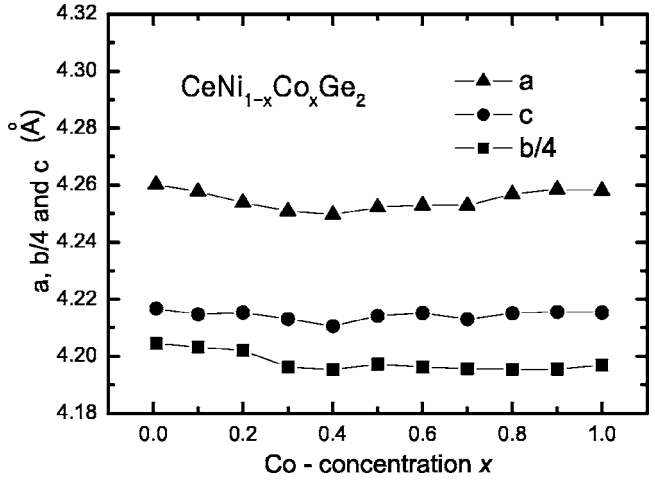

FIG. 1. Lattice parameters a, b, and c versus Co concentration x. Here, b is plotted as divided by 4 for better presentation.

behavior appears: (i) linear-T resistivity; (ii) $\sqrt{T}$ dependence in χ; and (iii) $-\ln T$ in C_p, suggesting that $x=0.3$ is a quantum critical point. The NFL behavior is consistent with that arising from two-dimensional antiferromagnetic quantum fluctuations. Preliminary results of magnetic susceptibility and specific heat of these compounds were reported in Ref. 16.

II. EXPERIMENTAL DETAILS

Polycrystalline samples of $CeNi_{1-x}Co_xGe_2$ $(0 \leqslant x \leqslant 1)$ were prepared by arc melting under argon atmosphere and annealed at 900 °C for three weeks inside an evacuated quartz tube. High purity starting materials were used; lanthanum and cerium (99.9%), cobalt and nickel (99.95%), and germanium (99.999%). Less than 0.3% weight loss occurred during the melting process. Metallographic analysis indicated that the samples used in this study were in single phase. A powder x-ray diffraction pattern showed that the crystal structure is orthorhombic $CeNiSi_2$-type (space group *Cmcm*). For the whole concentration range, the lattice parameters of a, b, and c remain almost unchanged (see Fig. 1). For $x<0.3$, where the lattice parameters are slightly decreased with increasing x, the volume change $[V(x)-V(x=1)]/V(x=1)$ is still less than 0.5%. On the other hand, large volume change $(\sim 10\%)$ was often observed for other well-studied systems such as $Ce(Pd_{1-x}Ni_x)_2Ge_2$,[17] $CeNi_2(Ge_{1-x}Si_x)_2$,[17] $CeCu_{2-x}Ni_xSi_2$,[18] and $CeCu_{6-x}Au_x$.[19] The negligible doping effect on lattice parameters of $CeNi_{1-x}Co_xGe_2$ indicates that chemical pressure effects are small and, consequently, the change in physical properties with doping concentration x probably arises from the difference of electron density between Ni and Co ions.

Magnetic susceptibility was measured using a superconducting quantum interference device (SQUID) magnetometer (MPMS5XL, Quantum Design, Co., Ltd.) from 2 to 300 K at $H=0.1$ T. Specific heat was measured by a relaxation method with a physical property measurement system (PPMS9, Quantum Design) from 2 to 200 K. A homemade

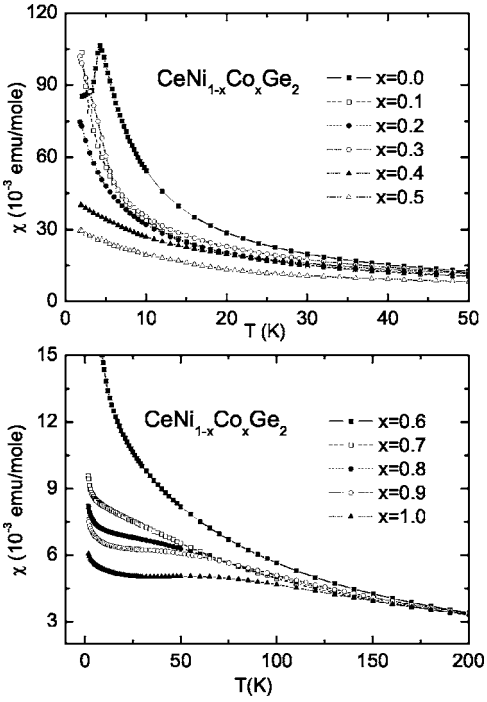

FIG. 2. Temperature dependence of the magnetic susceptibility $\chi(T)$ for $CeNi_{1-x}Co_xGe_2$.

^{3}He refrigerator was used to measure specific heat below 1.8 K via adiabatic method. Electrical resistivity was measured by a conventional dc four-probe method from 0.5 to 300 K using the homemade ^{3}He refrigerator. In order to correct errors that may occur in determining dimensions of the samples, the van der Pauw method was additionally used at 300 K in the resistivity measurement.

III. EXPERIMENTAL RESULTS AND ANALYSIS

A. Magnetic susceptibility

Figure 2 shows magnetic susceptibility $\chi(T)$ of $CeNi_{1-x}Co_xGe_2$ $(0 \leqslant x \leqslant 1)$ as a function of temperature from 2 to 300 K. At $x=0$, there are two peaks at 3.2 and 4.2 K due to antiferromagnetic phase transitions, consistent with single crystal results.[13] For $x \geqslant 0.1$, they are suppressed below 2 K and the absolute values of $\chi(T)$ decrease with increasing x. For $x>0.7$, $\chi(T)$ exhibits a weak maximum near 50 K and tends to saturate at lower temperatures before showing an upturn below 15 K. Such an upturn is often observed in Ce-based intermetallic compounds with high Kondo temperature T_K and is ascribed to a small amount of magnetic impurity or inhomogeneity induced from free Ce^{3+} and/or Co^{2+} ions.[20] This proposition was supported by the observation that the low-temperature upturn strongly depends on annealing condition. Assuming that only Co ions contribute to the upturn of $\chi(T)$ at low temperatures, we estimate the impurity concentration n by using a Curie from

$$\chi(T) = a + nC/T, \tag{1}$$

where C is the $j=9/2$ free-ion Curie constant and a is a fitting parameter. Best results were obtained with $n=0.06 \sim 0.08$ at. % Co impurities for $x>0.6$.

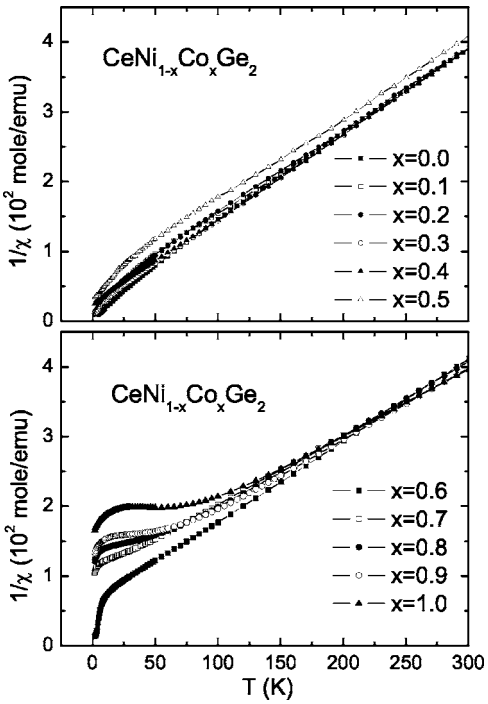

FIG. 3. Temperature dependence of the inverse magnetic susceptibility $1/\chi(T)$ for $CeNi_{1-x}Co_xGe_2$.

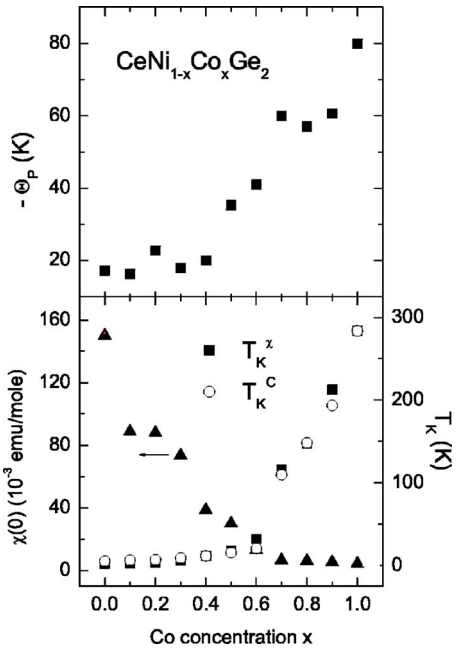

FIG. 4. (Upper panel) Paramagnetic Curie temperature Θ_p. (Lower panel) Kondo temperature T_K^{χ} and $\chi(0)$ evaluated from the magnetic susceptibility $\chi(T)$ and Kondo temperature T_K^C evaluated from $4f$ specific heat C_{4f} as a function of Co concentration x in $CeNi_{1-x}Co_xGe_2$.

Figure 3 displays the temperature dependence of the inverse magnetic susceptibility $1/\chi(T)$ of $CeNi_{1-x}Co_xGe_2$. At high temperature ($T>200$ K), $1/\chi$ linearly depends on T for all x values, which is well fitted by a Curie-Weiss law with an additional term χ_0 from temperature-independent van Vleck-type contributions

$$\frac{1}{\chi(T)-\chi_0}=\frac{T-\Theta_p}{C}, \tag{2}$$

where C is the Curie constant and Θ_p is the paramagnetic Curie temperature. Compared to the contribution from the localized moment, the χ_0 is negligibly small, ranging between 1.7×10^{-4} and 2.2×10^{-4} emu/mol. All compounds studied here have an effective moment μ_{eff} of approximately $2.55\mu_B$, which corresponds to the full Ce^{3+} moment and integer valence (+3) at high temperature. This result is consistent with Ref. 16, but is different from Ref. 14 that claimed an intermediate valence. In the upper panel of Fig. 4, paramagnetic Curie temperature Θ_p is plotted as a function of doping level x. It varies from -18 to -80 K for $x=0$ and $x=1$, respectively, indicating that antiferromagnetic exchange interactions become enhanced with increasing x. Since Θ_p is often a measure of the Kondo interactions in the Kondo system,[20] T_K may be enhanced with increasing x. It is interesting to note that a sudden change of slope seems to occur near $x=0.5$.

Below 200 K, the inverse magnetic susceptibility deviates from the linear T dependence. For $x\leqslant0.5$, this deviation is weak and seems arising from crystalline electric field effects. On the other hand, the deviation is relatively stronger for $x>0.5$: A shoulder appears near 20 K for $0.5<x\leqslant0.8$, and even a weak peak appears near 25 K for $x\geqslant0.9$. These features cannot be explained by crystalline electric field effects and require further explanation. Figure 5 shows corrected magnetic susceptibility χ_c after subtracting the impurity contribution that caused the low-T upturn. At $x=1$, χ_c is saturated to 4.43×10^{-3} emu/mol as T goes to 0 K and a broad maximum around 50 K is more pronounced after the background subtraction.[15] A similar peak is also observed for $x>0.6$, but is gradually weakened with decreasing x. The peak temperature decreases with decreasing x and finally disappears for $x\leqslant0.6$. These features can be explained by orbital effects within the Coqblin-Schrieffer (CS) model with different j, where j is the total angular momentum.[21,22] For each value of j, $\chi(T)/\chi(0)$ shows universal scaling against T/T_0, where T_0 is a characteristic energy scale that is related to Kondo temperature T_K through the Wilson number w, i.e, $T_K=wT_0$.[23] The experimental data are compared with the numerical solution[22] (solid lines) in Fig. 5, where j, T_0, and $\chi(0)$ were used as fitting parameters. The good agreement between the CS model and the experimental data underlines the importance of Kondo interactions in $CeNi_{1-x}Co_xGe_2$.

Different value of j were used for different ranges of x: $j=5/2$ for $x\geqslant0.9$, $j=3/2$ for $0.7\leqslant x\leqslant0.8$, and $j=1/2$ for $x\leqslant0.6$. The bottom panel of Fig. 4 shows $\chi(0)$ and T_K^{χ} as a function of doping concentration x, where T_K^{χ} is the Kondo temperature obtained from magnetic susceptibility χ. T_K^{χ} increases with increasing x and shows a sharp increase near $x=0.6$. This feature is related to a sharp increase in Θ_p at the similar doping concentration because both T_K and Θ_p are a measure of Kondo interactions. According to the CS model,[22] $\chi(0)\propto N(N^2-1)/T_K$, where $N=2j+1$. Even though $\chi(0)$ decreases with increasing x, there is no such sharp feature in $\chi(0)$ near $x=0.6$ as in T_K. The lack of feature in $\chi(0)$

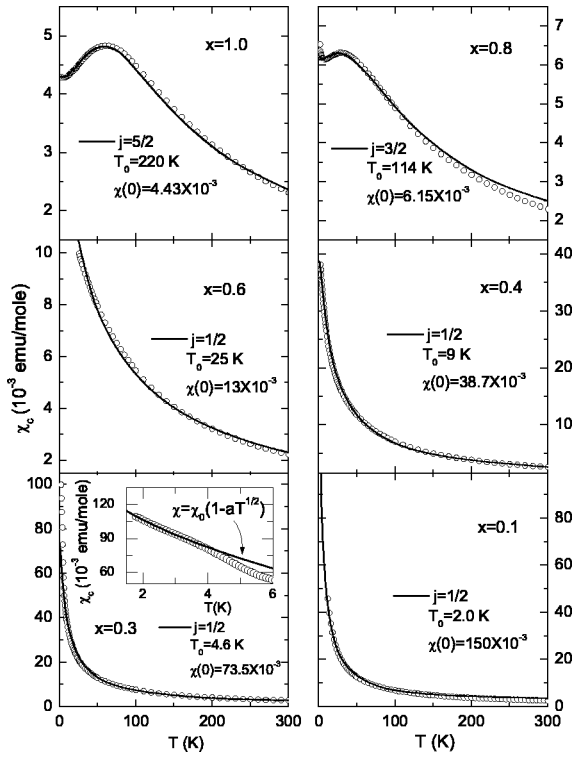

FIG. 5. Corrected magnetic susceptibility $\chi_c(T)$ of $CeNi_{1-x}Co_xGe_2$ by using the method mentioned in the text. The calculated results (solid line) from the Coqblin-Schrieffer model with various j values are also included. The inset in the graph for $x=0.3$ shows a power-law temperature dependence of the susceptibility, $\chi=\chi_0(1-aT^{1/2})$, in low temperature region. (See the text.)

may be related to large error bars or a change in the total angular momentum j with x. Finally, we note that at $x=0.3$, a deviation from the CS model occurs below 3.5 K. The low-T $\chi(T)$ shows a power-law dependence, $\chi_c=\chi_0(1-aT^{1/2})$, which has been considered as one of the hallmarks of non-Fermi liquid behavior. This NFL behavior in χ will be discussed in detail in Sec. IV.

B. Specific heat

Figure 6 shows C/T of $CeNi_{1-x}Co_xGe_2$ between 0.5 and 150 K on a semilog scale. For $x=0$, two peaks are observed at 3.40 and 2.84 K, which correspond to the two-step antiferromagnetic transitions as reported earlier.[13–15] With increasing x, the two peaks are merged to one, i.e., to 1.95 K at $x=0.1$. On further increasing x, no anomaly is found down to 0.5 K, indicating that the antiferromagnetic transition temperature is suppressed to zero near $x=0.3$, which is consistent with magnetic susceptibility. The Sommerfeld coefficient γ was estimated from the low-temperature C/T. As shown in Fig. 7, the linear specific heat coefficient is large for the whole concentration range, but strongly depends on the Co concentration. It rapidly increases with increasing x for $x<0.3$, while it gradually decreases with x for $x>0.3$. At $x=0.3$, γ diverges and C/T follows $-\ln T$ dependence below 6 K. This logarithmic temperature dependence of C/T, which is a characteristic feature of non-Fermi-liquid phenomena, strongly suggests that $x=0.3$ is a quantum critical point.

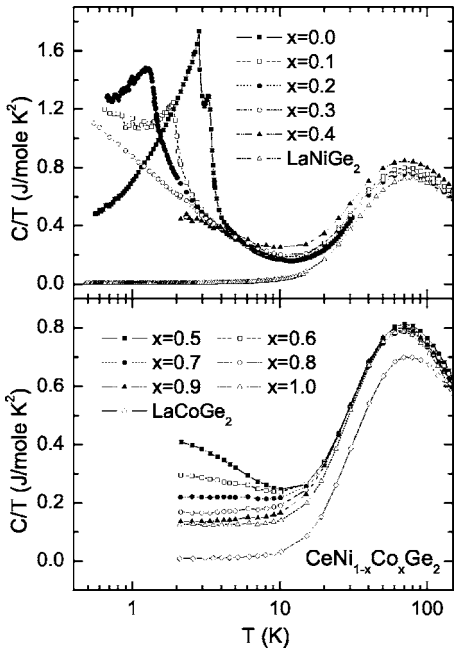

FIG. 6. Specific heat divided by temperature C/T for $LaNiGe_2$ and $LaCoGe_2$ as well as $CeNi_{1-x}Co_xGe_2$.

Figure 8 shows the magnetic specific heat, i.e, $C_{4f}=C(CeNi_{1-x}Co_xGe_2)-C(LaNi_{1-x}Co_xGe_2)$, where the specific heat of the nonmagnetic counterpart $LaNi_{1-x}Co_xGe_2$ was subtracted. For $0.4\leqslant x\leqslant 1$, C_{4f} exhibits a broad peak, which moves toward a lower temperature with decreasing x. The broad peak at $x=1$ can be explained by the Coqblin-Schrieffer (CS) model with $j=5/2$ and $T_0=220$ K (see top panel of Fig. 8),[15,22] suggesting that the crystalline-electric-field (CEF) splitting is negligible compared to large Kondo fluctuations. For $0.7\leqslant x\leqslant 0.9$, the experimental data are smaller than the result calculated by the CS model for $j=5/2$ but are larger than that for $j=3/2$ (see top panel of Fig. 8), indicating that the CEF splitting is comparable to the Kondo temperature. A numerical solution for a degenerate Kondo model, where $j=5/2$ multiplet splits into three

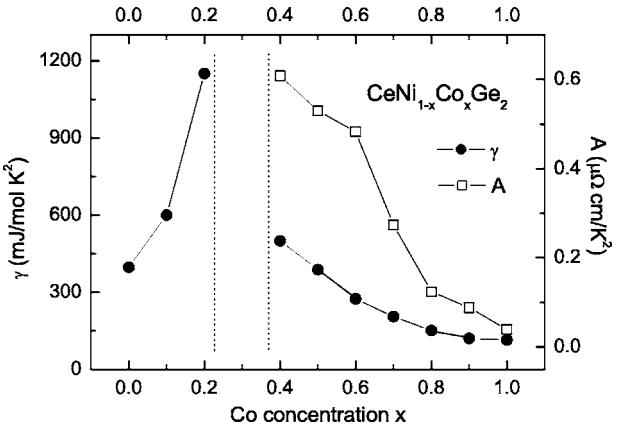

FIG. 7. Sommerfeld coefficient γ and the T^2 resistivity coefficient A as a function of Co concentration x in $CeNi_{1-x}Co_xGe_2$.

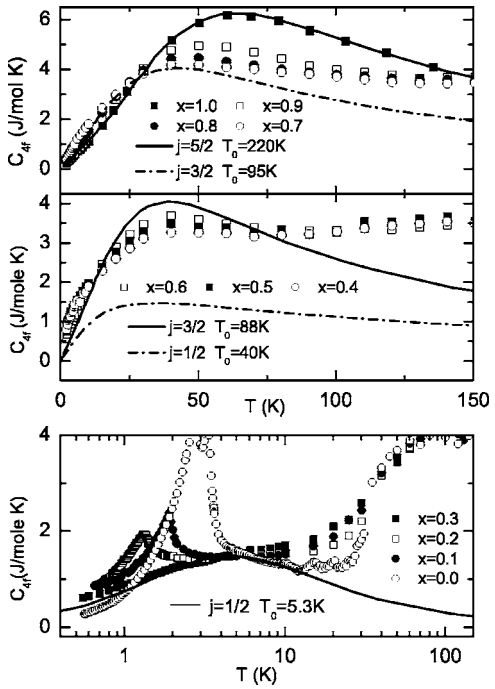

FIG. 8. $4f$-electron contribution to the specific heat C_{4f} given by the difference between the specific heats of $CeNi_{1-x}Co_xGe_2$ and $LaNi_{1-x}Co_xGe_2$. The solid lines indicate C_{4f} calculated from the Coqblin-Schrieffer model with various j values.

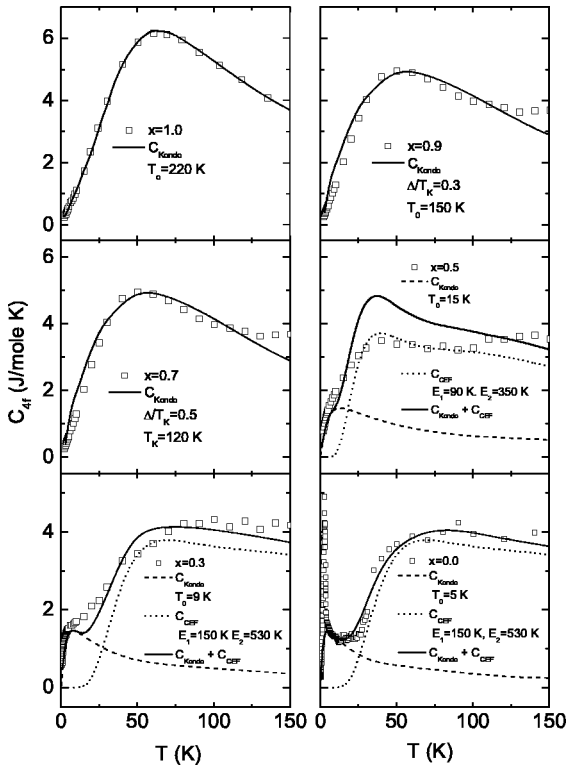

FIG. 9. C_{4f} data of $CeNi_{1-x}Co_xGe_2$ and the calculated results (solid line) from the Coqblin-Schrieffer model in the presence of crystalline electric field. The details are mentioned in the text.

equally spaced doublets separated by an energy Δ, have been reported by Desgranges and Rasul.[24] Although the CEF splitting scheme applied in their model may be different from ours, where the splitting energies may be unequal, the difference can be ignored if $\Delta/T_K < 0.5$. Figure 9 compares the experimental data and the numerical calculation (solid lines) based on the CS model with the equally spaced CEF splitting.[24] Best results were obtained with parameters as follows: $\Delta/T_K = 0.3$ and $T_K = 193$ K for $x = 0.9$, $\Delta/T_K = 0.47$ and $T_K = 148$ K for $x = 0.8$, and $\Delta/T_K = 0.53$ and $T_K = 120$ K for $x = 0.7$. These results suggest that the Kondo temperature at $x = 0.9$ is larger than the crystal field splitting energy ($2\Delta = 116$ K) but the T_K's at $x = 0.8$ and 0.7 are of same order or slightly smaller than 2Δ.

For $0.4 \leqslant x \leqslant 0.6$ (see middle panel of Fig. 8), the Kondo solution mentioned above cannot be applied because Δ/T_K is expected to be larger than 0.5. When we apply the $j = 3/2$ degenerate Kondo result calculated by Rajan,[22] our data are lower than the calculated values at the broad peak temperature (40 K), while they are higher than the calculated values at the shoulder near 10 K. We conjecture that the broad peak is related to CEF effects, while the shoulder is due to $j = 1/2$ Kondo state. In the middle-right panel of Fig. 9, we show the specific heat obtained from the $j = 1/2$ CS model (dashed line) C_{Kondo} and the Schottky anomaly with $E_1 = 90$ K and $E_2 = 480$ K (dotted line) C_{CEF} for $x = 0.5$, where E_1 and E_2 are the first and second excited doublets, respectively. The total specific heat (solid line), $C_{\text{total}} = C_{\text{Kondo}} + C_{\text{CEF}}$, correctly describes the broad peak and the shoulder, but the absolute values are overestimated near the broad peak (40 K). For $x \leqslant 0.3$ (see bottom panels of Fig. 9), the separate treatment for Kondo effects and CEF effects reproduces the data well with $E_1 = 150$ K and $E_2 = 530$ K. Kondo temperatures obtained from the fitting results are plotted in the bottom panel of Fig. 4, which was denoted as T_K^C (circles). The T_K^C's from the specific heat agree well with the T_K^χ's from the magnetic susceptibility, indicating that the conjecture used for the specific heat analysis for $x < 0.6$ is reasonable.

C. Electrical resistivity

The electrical resistivity $\rho(T)$ of $CeNi_{1-x}Co_xGe_2$ is shown in Fig. 10. As is often observed in Kondo compounds with high T_K,[25] a broad peak is observed at 120 and 90 K for $x = 1$ and 0.9, respectively. The magnetic part of the resistivity of $CeCoGe_2$ ρ_m, which was obtained by subtracting the ρ of $LaCoGe_2$, shows $-\ln T$ temperature dependence above the peak position, a signature of Kondo effects (see inset to the bottom panel of Fig. 10). The maximum, which is often interpreted as the coherence peak, moves toward a lower temperature with decreasing x down to $x = 0.4$, indicating the decrease in Kondo interactions. The decrease in T_K is consistent with the doping dependence of the T_K's obtained from the magnetic susceptibility and the specific heat analysis. For $x < 0.3$, the maximum splits into two maxima because T_K becomes comparable to the CEF splitting energy.[26] The inset in the top panel of Fig. 10 shows the magnetic resistivity of $CeNiGe_2$ that reveals $-\ln T$ dependence in two different temperature regions. Such behavior is expected for Kondo-type interactions in the presence of crystal field effects.[27] The ra-

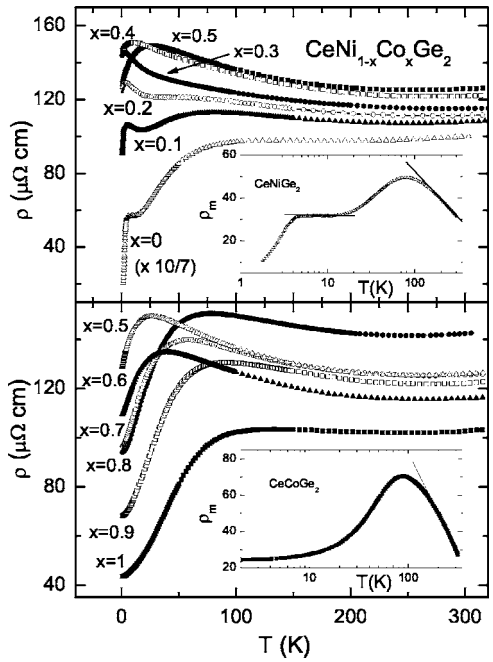

FIG. 10. Temperature dependence of the electrical resistivity $\rho(T)$ for $CeNi_{1-x}Co_xGe_2$. The insets show magnetic contribution to the resistivity for $CeNiGe_2$ and $CeCoGe_2$.

tio of the low- and high-temperature slopes are given by $(g_1{}^2-1)/(g_2{}^2-1)$, where g_1 and g_2 are the degeneracy of the $4f$ states at low and high temperatures, respectively. For $CeNiGe_2$, the ratio is estimated to be about 1/5, which corresponds to $g_1=2$ and $g_1=4$. This indicates that the low-temperature logarithmic region represents the Kondo effects from the CEF ground doublet, whereas the high-temperature region represents the Kondo effects due to the lowest two doublets. These regions are separated by a maximum whose temperature corresponds approximately to the CEF splitting. The resistivity data suggest a crystal field splitting of ~120 K for the first excited doublet, which is comparable to that obtained from specific heat data.

Figure 11 shows the low-temperature part of $\rho(T)$. For $x<0.3$, a sudden change in the resistivity slope occurs at 3.5 K ($x=0$), 2 K ($x=0.1$), and 1.6 K ($x=0.2$), due to the antiferromagnetic transitions observed in the specific heat and magnetic susceptibility measurements. At the critical concentration $x=0.3$, we could not observe any evidence for the antiferromagnetic (AF) transition within our experimental resolution down to 500 mK. Instead, $\rho(T)$ shows a linear temperature dependence for more than a decade, a key signature of non-Fermi liquid behavior. For $x\geq 0.4$, conventional Landau-Fermi-liquid behavior appears, i.e., $\rho=\rho+AT^2$. As x increases, the temperature range satisfying the Fermi-liquid behavior is extended, while the T^2 resistivity coefficient A is decreased due to enhanced Kondo effects (see Fig. 7)

IV. DISCUSSION

A. Various Kondo states

Heavy-fermion systems exhibit low-energy excitations for coherent Fermi-liquid behavior. Such behavior is most revealing in resistivity, which varies as T^2 below coherence temperature or Fermi-liquid temperature T_{FL}. In the top panel of Fig. 12, T^2 coefficient A of $CeNi_{1-x}Co_xGe_2$ is plotted against γ on a log-log scale, namely, the Kadowaki-Woods plot.[28] The value of A/γ^2 is close to the universal ratio $1\times 10^{-5}\mu\Omega$ cm mol^2 K^2 mJ^{-2} (solid line). The Wilson plot of $\chi(0)$ and γ, another characteristic plot for heavy-fermion compounds, is also shown on a log-log scale in the bottom

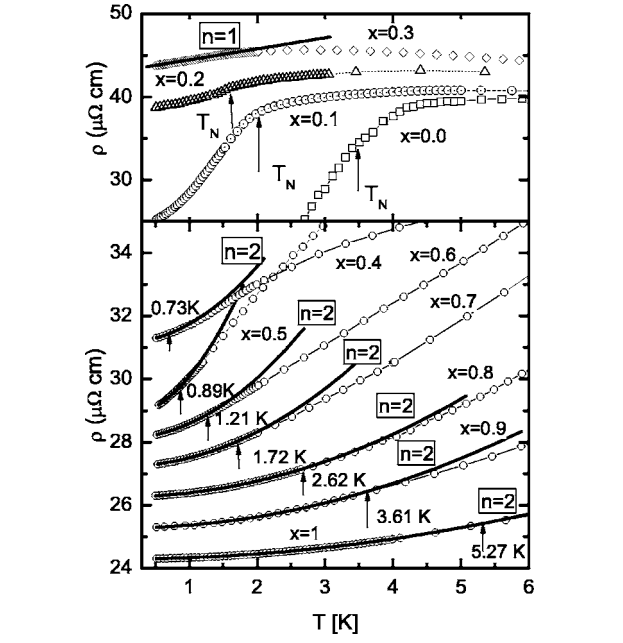

FIG. 11. Low-temperature parts of $\rho(T)$ for $CeNi_{1-x}Co_xGe_2$. The values are shifted for easy comparison with each other. (Upper panel) The solid line indicates the fitting curve of $\rho=\rho_0+\beta T$ and the arrows indicate the antiferromagnetic transition temperature T_N. (Lower panel) The solid lines indicate the fitting curves with $\rho=\rho_0+AT^2$ and the arrows indicate the maximum temperature T_{FL} of the T^2 dependence.

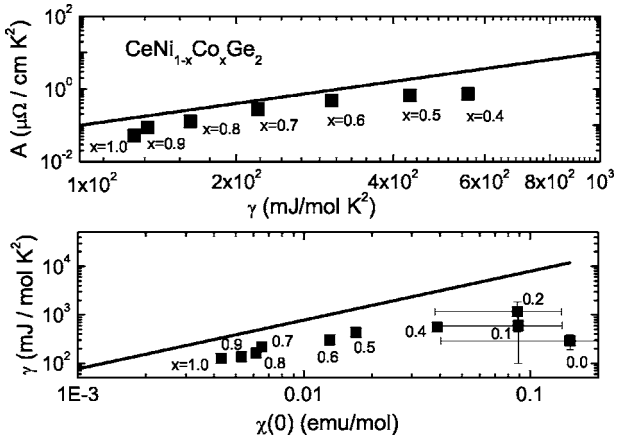

FIG. 12. (Upper panel) The T^2 resistivity coefficient A versus Sommerfeld coefficient in $CeNi_{1-x}Co_xGe_2$. The slope of A/γ in the logarithmic scale is nearly constant. (Lower panel) The Sommerfeld coefficient γ versus zero-temperature susceptibility $\chi(0)$ in $CeNi_{1-x}Co_xGe_2$. The slope of $\gamma/\chi(0)$ in the logarithmic scale is nearly constant. Symbols are for our samples.

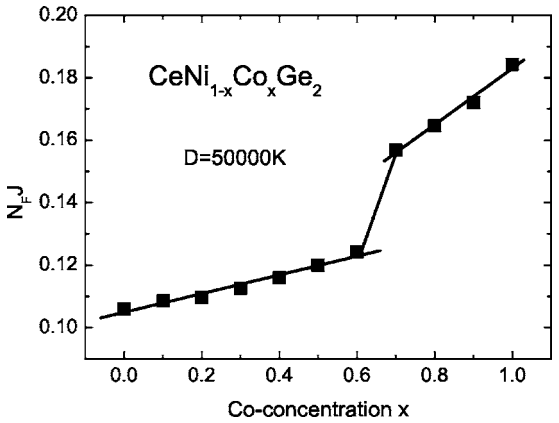

FIG. 13. Dimensionless effective exchange coupling constant $N_F J$ estimated from the equation of $T_K = D\exp(-1/N_F J)$, assuming $D = 5\times10^4$ K.

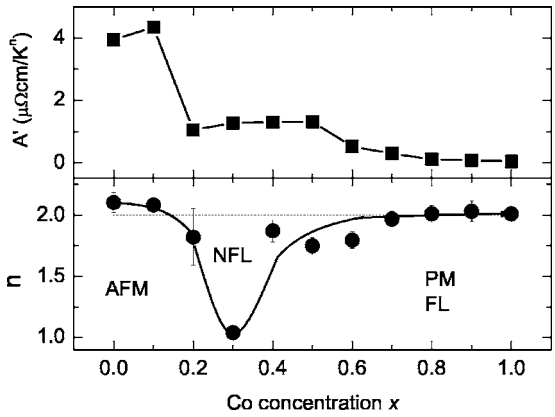

FIG. 14. Prefactor A' and the temperature exponent n as a function of Co concentration x.

panel of Fig. 12. The Wilson ratio $\gamma/\chi(0)$ for most of the concentration range x is in good agreement with the universal ratio expected for usual heavy-fermion systems (solid line). For $x<0.3$, the AF magnetic order makes it difficult to obtain precise values of such physical parameters as A, γ, and $\chi(0)$, leading to large error bars in the Kadowaki-Woods and Wilson ratio.

Figure 13 shows Co-concentration dependence of the dimensionless effective exchange coupling constant JN_F that was calculated through $T_K = D\exp(-1/JN_F)$,[22] where T_K is the averaged Kondo temperature, i.e., $T_K = (T_K^C + T_K^\chi)/2$. The prefactor D is related to the conduction-electron band width and is assumed to be constant (5×10^4 K) over the whole Co-concentration range. The effective coupling constant JN_F is linearly proportional to x up to 0.6, sharply increases at $x=0.6$, and increases with a relatively large slope for $x>0.6$. Similar to Ce monopnictides (CeX) where p-f mixing increases the p holes,[29] the doping dependence of JN_F is most likely due to the hybridization between the Ce $4f$ and Co/Ni $3d$ electrons because the change in x is expected to affect only $3d$ bands near the Fermi level. For $CeNi_{1-x}Co_xGe_2$, the lattice parameters are essentially independent of x, and thus the enhancement of hybridization with x most likely comes from a change in the electron density of states. To be more specific, Co substitution increases $3d$ electron states at the Fermi level because Co has one less $3d$ electron than Ni. Recently, reflectivity measurements show that the plasma edge in $CeCoGe_2$ is 5% higher than that in $CeNiGe_2$,[30] which is consistent with our proposition.

The sharp increase in JN_F near 0.6 may be related to a change in the effective degeneracy number $N(=2j+1)$, i.e., $j=1/2$ for $x\leqslant0.6$ and $j=3/2$ for $x>0.6$. In CeSb,[29] the p-f mixing of Ce $4f$-Γ_8 (Γ_8: the CEF excited state) with the Sb $5p$ state is sufficiently larger than that of Ce $4f$-Γ_7 (Γ_7: the ground state), leading to a decrease in the crystal field splitting between Γ_7 and Γ_8. A similar analysis can be applied to $CeNi_{1-x}Co_xGe_2$. Specific heat shows that the crystal field splitting tends to decrease with increasing x and sharply decreases for $x\geqslant0.6$, suggesting that the hybridization between the Ce $4f$ excited states and the Co $3d$ states becomes dominant for larger x, leading to the steep increase in JN_F at $x=0.6$.

B. Non-Fermi-liquid behavior

In the previous analysis, we have shown a plethora of experimental evidence that the non-Fermi-liquid state is realized in $CeNi_{1-x}Co_xGe_2$ at the critical concentration $x=0.3$. The low-temperature resistivity is best described by $\rho=\rho_0+A'T^n$ with $n=1\pm0.02$ (see Fig. 14). The specific heat divided by temperature C/T increases logarithmically with decreasing temperature at $x=0.3$ (see the top panel of Fig. 6). The magnetic susceptibility shows a power-law T dependence at low temperature, i.e., $\chi=\chi_0(1-aT^{1/2})$ (see inset to the bottom-left panel of Fig. 5). What could be the origin for the deviation from the Fermi-liquid state? Large residual resistivity at $x=0.3$, one order of magnitude higher than that of $CeNiGe_2$, suggests that the NFL phenomena observed in $CeNi_{1-x}Co_xGe_2$ may be associated with disorder effects.[31,32] However, we note that the linear specific-heat coefficient (C/T) of the nonstoichiometric alloys for $x>0.4$ agrees well with that evaluated from the Coqblin-Schrieffer model as analyzed before, indicating that the Kondo disorder is unlikely to be an important mechanism for the NFL behavior in our system.

It has been recently proposed that most of the NFL behavior in heavy Fermion systems may be explained in terms of a Griffiths phase. Simply speaking, the Griffiths phase is an inhomogeneous magnetic phase, similar to spin glass phase at a microscopic level.[11,12] It is conceivable that the spin glass phase exists in nonstoichiometric alloys. For the Griffiths phase, the specific heat coefficient C/T and susceptibility χ are expected to show power-law T dependence, i.e., $C/T\propto\chi\propto T^{-1+\lambda}$ with $\lambda<1$ in the NFL regime. In $CeNi_{1-x}Co_xGe_2$ with $x=0.3$, C/T was best described with $\lambda_C=0.6$ in a temperature region of 0.5 K$<T<$1.2 K and χ, with $\lambda_\chi=0.72$ for 1.8 K$<T<$2.5 K. However, it is impossible to describe both the specific heat and susceptibility with the same λ, arguing against the Griffiths phase scenario.

The fact that the NFL behavior appears at the critical concentration $x=0.3$ where the AF magnetic order is suppressed to 0 K strongly suggests that $x=0.3$ is a quantum critical point. As we dope Co to the Ni site in $CeNi_{1-x}Co_xGe_2$, the ordered AF ground state changes to a nonmagnetic disordered state at $T=0$ K, crossing the quantum critical point.

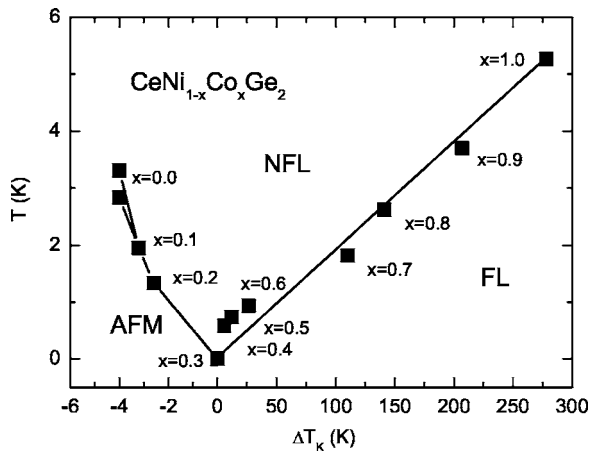

FIG. 15. Phase diagram as a function of $\Delta T_K = T_K(x) - T_K$ ($x = 0.3$) in $CeNi_{1-x}Co_xGe_2$.

There has been theoretical consideration on how the dimensionality of quantum fluctuations affects thermodynamic and transport properties in the NFL state.[8,9] When three-dimensional (3D) conduction electrons are coupled to 3D AF fluctuations $\rho = \rho_0 + A'T^{3/2}$, $C/T = \gamma_0 - \alpha\sqrt{T}$, and $\chi \propto T^{3/2}$. For 2D AF fluctuations, on the other hand, slightly different temperature dependence is expected: $\rho = \rho_0 + A'T$, $C/T = c\ln(T_0/T)$ and $\chi = \chi_0 - aT$. The linear T dependence in ρ and the $-\ln T$ in C/T of $CeNi_{1-x}Co_xGe_2$ ($x = 0.3$) favor the 2D AF fluctuations over the 3D fluctuations. It has been argued that the 3D spin-fluctuation model with additional coupling between the spin-fluctuation modes can give rise to similar results to the 2D model below a crossover temperature T^*: $C/T \propto \sqrt{T}$ and $\rho \propto T^{3/2}$ for $T < T^*$, while $C/T \propto -\ln T$ and $\rho \propto T$ for $T > T^*$.[8,9] The absence of the crossover temperature T^* and the strong magnetic anisotropy reported in Ref. 13 underlines the importance of 2D AF fluctuations at $x = 0.3$.

Further support to the 2D AF fluctuations comes from the T_K dependence of the AF transition temperature T_N and the Fermi-liquid temperature T_{FL} where a crossover from FL to NFL occurs. Figure 15 shows the phase diagram of T_N and T_{FL} as a function of relative Kondo temperature $\Delta T_K = T_K(x) - T_K(x = 0.3)$. A quantum phase transition predicts that $T_{FL} \propto (\delta - \delta c)$ and $T_N \propto (\delta - \delta c)^{2/3}$ for 3D AF fluctuations and $T_{FL} \propto (\delta - \delta c)$ and $T_N \propto (\delta - \delta c)$ for 2D fluctuations, where δ and δ_c are the tuning parameter and critical point, respectively.[8,9] In this analysis, T_K was used as a tuning parameter because the lack of change in the lattice constants with Co doping x suggests that T_K is a more relevant control parameter than x. T_{FL} linearly increases with ΔT_K, while T_N shows an exponent of $|\Delta T_K|$, higher than 2/3 for 3D, but close to 1 for 2D AF fluctuations, which is consistent with the conclusion drawn both from thermodynamic and transport measurements. For a definite conclusion, experimental studies such as neutron scattering are required.

V. CONCLUSION

We have studied various ground states that occur due to competiion between Kondo and RKKY interaction in $CeNi_{1-x}Co_xGe_2$. The RKKY exchange interaction is dominant for $x < 0.3$, leading to local moment magnetism with negligible Kondo screening. With increasing x, the antiferromagnetic transition temperature T_N is suppressed to 0 K at the critical concentration of $x = 0.3$. A further increase of x stabilizes the Fermi-liquid state, $\rho = \rho_0 + AT^2$, and consequently, Fermi-liquid temperature T_{FL} is extended. The phase diagram demonstrates that non-Fermi-liquid (NFL) behavior appears close to x_c, where weak power-law or logarithmic temperature dependences are observed: $\chi \propto \chi_0(1 - aT^{1/2})$, $\rho \propto \rho_0 + \beta T$, and $C/T \propto -\ln T$. We argue that the observed NFL state is due to a quantum phase transition coupled to 2D AF fluctuations. The low temperature data of the magnetic susceptibility and specific heat are well accounted for by the Coqblin-Schrieffer model with degenerate impurity spin $j = 1/2$ for $x \leqslant 0.6$, $j = 2/3$ for $0.6 < x < 0.9$, and $j = 5/2$ for $x \geqslant 0.9$.

ACKNOWLEDGMENTS

This work is supported by the Korea Science and Engineering Foundation through the Center for Strongly Correlated Materials Research (CSCMR) at Seoul National University and by Grant No. R01-2003-000-10095-0 from the Basic Research Program of the Korea Science and Engineering Foundation.

*Author to whom correspondence should be addressed; e-mail: yskwon@skku.ac.kr

[1] G. R. Stewart, Rev. Mod. Phys. **56**, 755 (1984).
[2] N. Grewe and F. Steglich, *Handbook on the Physics and Chemistry of Rare Earth* (Elsevier Science Publishers B. V., Amsterdam, 1991), Vol. 14.
[3] S. Doniach, Physica B & C **91**, 231 (1977).
[4] D. L. Cox, Phys. Rev. Lett. **59**, 1240 (1987); D. L. Cox and M. Jarrel, J. Phys.: Condens. Matter **8**, 9825 (1996).
[5] P. Schlottmann and P. D. Sacramento, Adv. Phys. **42**, 641 (1993).
[6] O. O. Bernal, D. E. MacLaughlin, H. G. Lukefahr, and B. Andraka, Phys. Rev. Lett. **75**, 2023 (1995); O. O. Bernal, D. E. MacLaughlin, A. Amato, R. Feyerherm, F. N. Gygax, A. Schenck, R. H. Heffner, L. P. Le, G. J. Nieuwenhuys, B. Andraka, H. v. Löhneysen, O. Stockert, and H. R. Ott, Phys. Rev. B **54**, 13000 (1996).
[7] E. Miranda, V. Dobrosavljevic, and G. Kotliar, J. Phys.: Condens. Matter **8**, 9871 (1996); Phys. Rev. Lett. **78**, 290 (1997).
[8] A. J. Millis, Phys. Rev. B **48**, 7183 (1993).
[9] T. Moriya and T. Takimoto, J. Phys. Soc. Jpn. **64**, 960 (1995).
[10] G. G. Lonzarich, in *Electron*, edited by M. Springford (Cambridge University Press, Cambridge, England, 1997).
[11] A. H. Castro Neto, G. Castilla, and B. A. Jones, Phys. Rev. Lett. **81**, 3531 (1998).

[12] R. B. Griffiths, Phys. Rev. Lett. **23**, 17 (1969).
[13] M. H. Jung, N. Harrison, A. H. Lacerda, H. Nakotte, P. G. Pagliuso, J. L. Sarrao, and J. D. Thompson, Phys. Rev. B **66**, 054420 (2002).
[14] V. K. Pecharsky and K. A. Gschneidner, Jr., Phys. Rev. B **43**, 8238 (1991).
[15] E. D. Mun, B. K. Lee, Y. S. Kwon, and M. H. Jung, Phys. Rev. B **69**, 085113 (2004).
[16] E. D. Moon, S. O. Hong, D. L. Kim, H. C. Ri, and Y. S. Kwon, Physica B **329–333**, 516 (2003).
[17] G. Knebel, M. Brando, J. Hemberger, M. Nicklas, W. Trinkl, and A. Loidl, Phys. Rev. B **59**, 12390 (1999).
[18] E. V. Sampathkumaran and R. Vijayaraghavan, Phys. Rev. Lett. **56**, 2861 (1986).
[19] A. Rosch, A. Schröder, O. Stockert, and H. v. Löhneysen, Phys. Rev. Lett. **79**, 159 (1997).
[20] N. B. Brandt and V. V. Moshchalkov, Adv. Phys. **33**, 373 (1984); J. Lawrence, Phys. Rev. B **20**, 3770 (1979).
[21] B. Coqblin and J. R. Schrieffer, Phys. Rev. **185**, 847 (1969).
[22] V. T. Rajan, Phys. Rev. Lett. **51**, 308 (1983); references therein.
[23] N. Andrei and J. H. Lowenstein, Phys. Rev. Lett. **46**, 356 (1981).
[24] H. U. Desgranges and J. W. Rasul, Phys. Rev. B **36**, 328 (1987).
[25] C. L. Lin, A. Wallash, J. E. Crow, T. Mihalisin, and P. Schlottmann, Phys. Rev. Lett. **58**, 1232 (1987); R. Pott, R. Schefzyk, and D. Wohlleben, Z. Phys. B: Condens. Matter **44**, 17 (1981).
[26] K. H. J. Buschow, H. J. Van Daal, F. E. Maranzana, and P. B. Van Aken, Phys. Rev. B **3**, 1662 (1971); A. Percheron, J. C. Achard, O. Gorochov, B. Cornut, D. Jerome, and B. Coqblin, Solid State Commun. **12**, 1289 (1973).
[27] B. Cornut and B. Coqblin, Phys. Rev. B **5**, 4541 (1972).
[28] K. Kadowaki and S. B. Woods, Solid State Commun. **58**, 507 (1986).
[29] H. Takahashi and T. Kasuya, J. Phys. C **18**, 2709 (1985); **18**, 2721 (1985).
[30] Y. S. Kwon (unpublished).
[31] P. Pedrazzini, M. Gómez Berisso, N. Caroca-Canales, M. Deppe, C. Geibel, and J. G. Sereni, Physica B **312–313**, 406 (2002).
[32] O. O. Bernal, D. E. MacLaughlin, H. G. Lukefahr, and B. Andraka, Phys. Rev. Lett. **75**, 2023 (1995); O. O. Bernal, D. E. MacLaughlin, A. Amato, R. Feyerherm, F. N. Gygax, A. Schenck, R. H. Heffner, L. P. Le, G. J. Nieuwenhuys, B. Andraka, H. v. Löhneysen, O. Stockert, and H. R. Ott, Phys. Rev. B **54**, 13000 (1996).